

# Vapor-phase selective aerobic oxidation of benzylamine to dibenzylimine over silica-supported vanadium-substituted tungstophosphoric acid catalyst

Cite this: *Green Chem.*, 2013, **15**, 837

K. T. Venkateswara Rao, B. Haribabu, P. S. Sai Prasad and N. Lingaiah\*

Silica-supported vanadium-substituted tungstophosphoric acid (TPAV<sub>x</sub>, x = 0–3) catalysts were prepared by an impregnation method and their physico-chemical properties derived from different spectroscopic techniques. The characterization results confirmed the incorporation of vanadium into the framework of heteropoly tungstate anion and the Keggin structure remained intact on SiO<sub>2</sub>. Vapor-phase aerobic oxidation of benzylamine was evaluated over these catalysts and dibenzylimine was obtained as the selective oxidative condensation product. Under optimized reaction conditions, 90% conversion of benzylamine with 95% selectivity to dibenzylimine was achieved over 20 wt% TPAV<sub>1</sub>/SiO<sub>2</sub> catalyst. The catalyst showed constant activity, after an initial decrease by about 10%, during the time on stream analysis. Controllable acidity and redox properties of the catalyst were accountable for high catalytic activity and selectivity. A plausible reaction mechanism is also elucidated.

Received 1st November 2012,

Accepted 24th January 2013

DOI: 10.1039/c3gc36735e

[www.rsc.org/greenchem](http://www.rsc.org/greenchem)

## 1. Introduction

Imines are important compounds with extensive applications in laboratory and industrial synthetic processes because of their unusual reactivity.<sup>1</sup> Traditionally, imines have been synthesized by condensation of aldehyde or ketone with amine in the presence of an acid catalyst. This approach has certain drawbacks associated with the excessive active nature of ketones/aldehydes. Nicolaou *et al.* established an organic reagent, 2-iodoxybenzoic acid (IBX), for the oxidation of amines to imines.<sup>2</sup> However, this reagent oxidizes secondary amines to imines. In the case of primary amines this reagent gave a carbonyl compound as final product instead of imine. Generally, the use of organic reagents produces large amounts of waste in the form of byproducts and also requires organic solvents as reaction media. Therefore, a less toxic and environmentally friendly process for the synthesis of imines is highly desirable. Catalytic aerobic oxidation of amines has received significant attention during the recent past. In this respect, various transition metal catalysts have also been proposed. Important examples include 10% PVMo/C,<sup>3</sup> gold,<sup>4–8</sup> ruthenium,<sup>9</sup> vanadium,<sup>10,11</sup> copper,<sup>12</sup> palladium,<sup>13</sup> TiO<sub>2</sub>,<sup>14</sup> Nb<sub>2</sub>O<sub>5</sub>,<sup>15</sup> carbon nitride,<sup>16</sup> and Fe<sup>3+</sup>-based MOFs.<sup>17</sup> All these catalysts are employed in liquid-phase conditions by using different

organic solvents. Besides, these approaches require prolonged reaction times to achieve desirable yields.

In fine chemical synthesis, selective vapor-phase oxidation reactions have more advantages than conventional liquid-phase reactions, particularly in industrial perspectives.<sup>18</sup> The liquid-phase processes necessitate additional steps for the purification of the product. They are expensive and environmentally not favorable. To the best of our knowledge there has been to date no report on selective vapor-phase oxidation of amines, in particular the oxidation of benzylamine to dibenzylimine. Thus, the development of a heterogeneous catalyst for selective vapor-phase aerobic oxidation of benzylamine is highly desirable.

Heteropoly acids (HPAs), especially Keggin-type, have been employed as promising catalysts for various oxidation and acid-catalyzed reactions.<sup>19,20</sup> HPAs possess special characteristics that make them very active in catalytic reactions. Vanadium-containing molybdophosphoric acid has been widely studied as catalyst for various oxidation reactions such as oxidation of isobutene,<sup>21</sup> methanol,<sup>22</sup> methacrolein,<sup>23</sup> propene,<sup>24</sup> propylene<sup>25</sup> and toluene.<sup>26</sup> 12-Tungstophosphoric acid (TPA), a highly acidic heteropoly acid, is modified with incorporation of V to shift its acid-dominated properties to a redox nature. Theoretically, vanadium atoms present in Keggin heteropoly acid leads to reduction of acidic strength while simultaneously enhancing the reoxidativity. There are a few catalytic applications reported on vanadium-containing tungstophosphoric acid catalyst such as oxidation of methanol,<sup>27</sup> alcohols,<sup>28</sup> bromination of olefins<sup>29</sup> and nitration

Catalysis Laboratory, I&PC Division, Indian Institute of Chemical Technology, Hyderabad 500 607, India. E-mail: [nakkalingaiah@iict.res.in](mailto:nakkalingaiah@iict.res.in); Fax: +91-40-27160921; Tel: +91-40-27193163

of phenol.<sup>30</sup> It is interesting to know how the modification of TPA with V results in the enhancement of oxidation ability. We have been working on modified Keggin heteropoly acids for different catalytic applications under liquid and vapor-phase conditions.<sup>31–36</sup>

In the present work, silica-supported vanadium-substituted tungstophosphoric acid ( $H_{3+x}PW_{12-x}V_xO_{40}$ ,  $x = 1-3$ ) catalysts were evaluated for vapor-phase selective aerobic oxidation of benzylamine to dibenzylimine. The influence of various reaction parameters was also studied. The catalytic activity was correlated with the observed characteristics of the catalysts.

## 2. Experimental

### 2.1. Preparation of vanadium-substituted tungstophosphoric acid catalysts

Vanadium-substituted TPA ( $H_4PW_{11}V_1O_{40}$ ; TPAV<sub>1</sub>) was prepared according to the method reported in the literature.<sup>37</sup> In a typical method, sodium metavanadate ( $NaVO_3$ , 7.33 mmol) was dissolved in 50 ml of deionized water at 80 °C and mixed with disodium hydrogen phosphate ( $Na_2HPO_4$ , 7.3 mmol), which had been previously dissolved in 20 ml of water. The mixture was cooled to room temperature and concentrated  $H_2SO_4$  (5 ml) was then added to give a red solution. Sodium tungstate dihydrate ( $Na_2WO_4 \cdot 2H_2O$ , 79.32 mmol) was dissolved in 50 ml of distilled water separately and the aqueous solution was added to the above red solution drop-wise with vigorous stirring followed by slow addition of concentrated  $H_2SO_4$ . The TPAV<sub>1</sub> formed was extracted with diethyl ether from the middle layer as heteropoly etherate. Subsequently the ether was removed by passing air through the solution. The yellow solid obtained was dissolved in water and concentrated until crystals appeared. Similarly, TPAV<sub>2</sub> ( $H_5PW_{10}V_2O_{40}$ ) and TPAV<sub>3</sub> ( $H_6PW_9V_3O_{40}$ ) catalysts were also prepared by varying the vanadium and tungsten contents of the starting materials.

A similar procedure was followed for the preparation of vanadium-containing molybdophosphoric acid (MPAV<sub>1</sub>) by taking  $Na_2MoO_4 \cdot 2H_2O$  as precursor for Mo.

### 2.2. Preparation of silica-supported TPAV<sub>x</sub> ( $x = 1-3$ ) catalysts

Silica (Cab-o-Sil, fumed form)-supported catalysts were prepared by an impregnation method. The required quantity of TPAV was dissolved in the minimum amount of water and this solution was added to the support with constant stirring. The excess water was removed on a hot plate and the catalyst masses were dried in an air oven at 120 °C for 12 h. The catalysts were finally calcined in air at 300 °C for 2 h. These catalysts were denoted as TPAV<sub>1</sub>/SiO<sub>2</sub>, TPAV<sub>2</sub>/SiO<sub>2</sub> and TPAV<sub>3</sub>/SiO<sub>2</sub>. The composition of active component (TPAV<sub>1</sub>, TPAV<sub>2</sub> and TPAV<sub>3</sub>) was fixed as 20 wt% for all the catalysts. Similarly 20 wt% MPAV<sub>1</sub>/SiO<sub>2</sub> and 20 wt% TPA/SiO<sub>2</sub> catalysts were also prepared for comparison.

### 2.3. Reaction procedure

Aerobic oxidation of benzylamine was carried out in a fixed-bed vertical glass reactor ( $h = 350$  mm,  $d = 12$  mm) under atmospheric pressure. In a typical experiment, about 0.5 g of the catalyst (crushed to a particle size of 18/25 BSS mesh to avoid mass transfer limitations) was diluted with the same size and volume of quartz beads and loaded into the reactor. Before starting the reaction the catalyst was pretreated in air at 300 °C for 1 h. The reaction was carried with flowing air (60 ml min<sup>-1</sup>) as oxidation medium. Benzylamine (2 ml h<sup>-1</sup>) was supplied through a syringe pump (B. Braun, Germany). The reaction was carried out at different temperatures in the range of 200–300 °C. After allowing the catalyst to attain a steady-state for 30 min at reaction temperature, the liquid product was collected for 30 min in a trap kept at –10 °C. The products were analyzed by gas chromatography, separating on a SE-30 column using a flame ionization detector (FID). The analysis of the non-condensable exit gas mixture was analyzed using GC with TCD and it was confirmed that there were no organic species or oxides of carbon in considerable range.

### 2.4. Catalyst characterization

Fourier transform infrared (FT-IR) spectra of catalysts were taken on a DIGILAB (USA) IR spectrometer using the KBr disc method. Powder X-ray diffraction (XRD) patterns of the catalysts were recorded on a Rigaku Miniflex (Rigaku Corporation, Japan) X-ray diffractometer using Ni-filtered Cu K $\alpha$  radiation ( $\lambda = 1.5406$  Å) with a scan speed of 2° min<sup>-1</sup> and a scan range of 10–80° at 30 kV and 15 mA.

Laser Raman spectra of the samples were collected with a Horiba-Jobin Yvon LabRam-HR spectrometer equipped with a confocal microscope, 2400/900 grooves per mm gratings, and a notch filter. The visible laser excitation at 532 nm (visible/green) was used. The scattered photons were directed and focused onto a single-stage monochromator and measured with a UV-sensitive LN<sub>2</sub>-cooled CCD detector. *In situ* Raman spectra of the catalyst was recorded using the same Raman spectrometer equipped with a high-temperature catalyst cell reactor (Linkam CCP 1000) using a 50× long working distance objective. The catalyst sample, typically about 10–15 mg of loose powder, was placed in an environmentally controlled high-temperature reactor cell containing a quartz window. The temperature of the reactor cell was controlled by a programmable temperature controller.

X-ray photoelectron spectroscopy (XPS) measurements were conducted on a KRATOS AXIS 165 with a dual anode (Mg and Al) apparatus using Mg K $\alpha$  anode. The non-monochromatized Al K $\alpha$  X-ray source ( $h\nu$  1486.6 eV) was operated at 12.5 kV and 16 mA. Before acquisition of the data, the sample was out-gassed for about 3 h at 100 °C under a vacuum of  $1.0 \times 10^{-7}$  Torr to minimize surface contamination. The XPS instrument was calibrated using Au as standard. For energy calibration, the carbon 1s photoelectron line was used. The carbon 1s binding energy was taken as 285 eV. A charge neutralization of 2 eV was used to balance the charge up of the sample. The

spectra were deconvoluted using a Sun Solaris-based Vision-2 curve resolver. The location and the full width at half-maximum (fwhm) value for the species were first determined using the spectrum of the pure sample. Symmetric Gaussian shapes were used in all cases.

Temperature-programmed desorption of ammonia (TPD of  $\text{NH}_3$ ) was carried out on a laboratory-built apparatus. In a typical experiment, about 0.1 g of the sample was pretreated at 300 °C for 1 h by passing helium (99.9%, 50 ml  $\text{min}^{-1}$ ). After pretreatment, the sample was saturated with anhydrous ammonia (10%  $\text{NH}_3$  balance He) at 100 °C for 1 h and subsequently flushed with He at the same temperature to remove physisorbed ammonia. Then the TPD analysis was carried out from ambient temperature to 800 °C at a heating rate of 10 °C  $\text{min}^{-1}$  and the desorbed  $\text{NH}_3$  was measured using a gas chromatograph equipped with a thermal conductivity detector.

### 3. Results and discussion

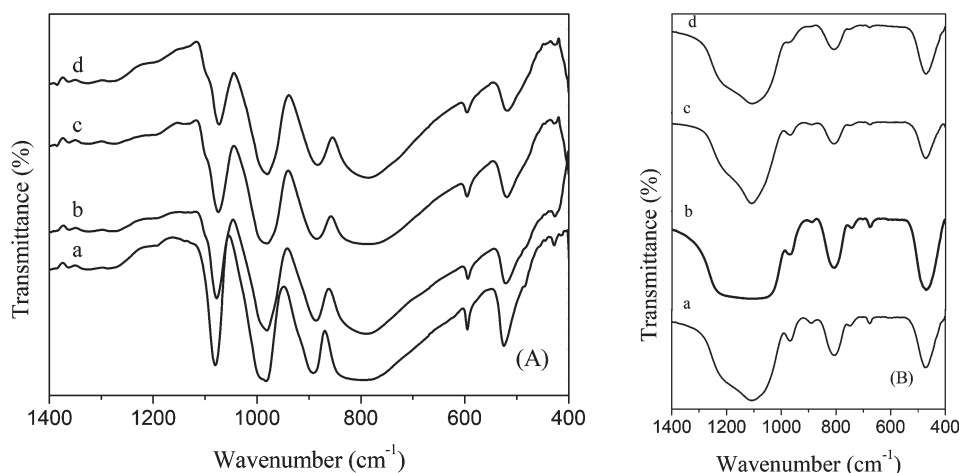
#### 3.1. FT-IR spectroscopy

Fig. 1A shows the FT-IR pattern of bulk  $\text{TPAV}_x$  ( $x = 1$  to 3) catalysts. The FT-IR spectrum of TPA is also included for comparison. Bulk TPA exhibited a FT-IR pattern in the range of 1100–700  $\text{cm}^{-1}$ . The characteristic Keggin ion peaks observed at 1082, 988, 890, 792 and 592  $\text{cm}^{-1}$  can be attributed to asymmetric vibrations of  $\text{P-O}_a$  ( $\text{O}_a$  denotes an oxygen atom bound to three W atoms and to P),  $\text{W=O}_t$  ( $t$  denotes the terminal oxygen),  $\text{W-O}_b\text{-W}$  ( $\text{O}_b$  denotes a corner-sharing bridging oxygen atom), and  $\text{W-O}_c\text{-W}$  ( $\text{O}_c$  denotes an edge-sharing bridging oxygen atom) and the bending mode of  $\text{O}_a\text{-P-O}_a$ , respectively.<sup>38</sup> The  $\text{TPAV}_x$  catalysts, in addition to the Keggin characteristic bands, showed a shoulder band at 1095  $\text{cm}^{-1}$ . This band corresponds to the asymmetric vibration of  $\text{P-O}_a\text{-V}$  bond.<sup>39</sup> The splitting of the  $\text{P-O}_a$  band is due to the introduction of a cation other than W into the Keggin structure, which induces a decrease in  $\text{W-O}_t$  stretching frequency, leading to

splitting of  $\text{P-O}_a$  band.<sup>40</sup> Incorporation of vanadium into primary structure of TPA led to a shift and/or splitting of the main FT-IR band due to reduced structural symmetry.<sup>41</sup> This confirmed the incorporation of vanadium into the primary structure of the Keggin ion. In the case of silica-supported catalysts (Fig. 1B), the main FT-IR bands observed at 1105  $\text{cm}^{-1}$  (strong and broad), 811  $\text{cm}^{-1}$  (medium) and 472  $\text{cm}^{-1}$  (strong) can be attributed to the presence of pure silica, as also reported in the literature.<sup>42</sup> One cannot distinguish the characteristic Keggin ion band at 1078  $\text{cm}^{-1}$  after impregnating  $\text{TPAV}_x$  on  $\text{SiO}_2$ . This is due to the strong absorption of silica in that region. However, the characteristic IR bands of Keggin ion were observed at 969 and 890  $\text{cm}^{-1}$ , indicating the presence of  $\text{TPAV}_x$  Keggin ion on the support. Thus, the IR results confirm the incorporation of vanadium into the primary structure of the heteropoly anion and its retention in the Keggin structure even after impregnation on silica.

#### 3.2. X-ray diffraction

Fig. 2 shows the XRD patterns of the catalysts. The patterns of bulk  $\text{TPAV}_x$  ( $x = 1$  to 3) were similar to that of parent TPA.<sup>43</sup> The Keggin structure was intact even with the incorporation of vanadium in the primary structure of heteropoly anion. Diffraction patterns corresponding to  $\text{TPAV}_x$  were not observed in the case of silica-supported catalysts, indicating that no crystalline phase related to  $\text{TPAV}_x$  ( $x = 1$  to 3) was formed on the  $\text{SiO}_2$  surface. This could be attributed to the interaction of the Keggin ion with the surface of silica as a result of uniform distribution. Alternatively, the  $\text{TPAV}_x$  might have existed on the  $\text{SiO}_2$  surface with particle size less than 4 Å, which is the detection limit of XRD. A similar observation was also made by Yadav and George<sup>44</sup> for  $\text{Cs}_{2.5}\text{H}_{0.5}\text{PW}_{12}\text{O}_{40}$  supported on mesoporous silica. However, a physical mixture of  $\text{TPAV}_1$  (20 wt%) and  $\text{SiO}_2$  showed the XRD patterns related to Keggin structure (data not shown). One important observation made from XRD was that no new crystalline phases were formed after impregnation of  $\text{TPAV}_x$  on  $\text{SiO}_2$ .



**Fig. 1** (A) FT-IR spectra of bulk (a) TPA, (b)  $\text{TPAV}_1$ , (c)  $\text{TPAV}_2$ , (d)  $\text{TPAV}_3$  catalysts. (B) FT-IR spectra of (a) 20  $\text{TPAV}_1/\text{SiO}_2$ , (b) 20  $\text{TPAV}_2/\text{SiO}_2$ , (c) 20  $\text{TPAV}_3/\text{SiO}_2$ , (d) 20  $\text{TPAV}_1/\text{SiO}_2$  (used) catalysts.

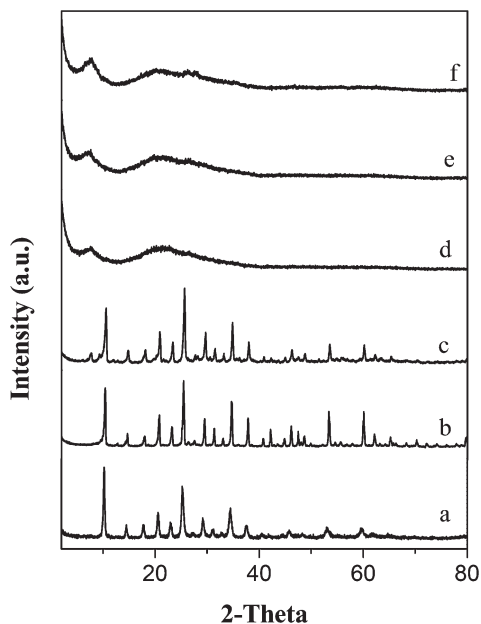


**Fig. 2** XRD patterns of (a) TPAV<sub>1</sub>, (b) TPAV<sub>2</sub>, (c) TPAV<sub>3</sub>, (d) 20 TPAV<sub>1</sub>/SiO<sub>2</sub>, (e) 20 TPAV<sub>2</sub>/SiO<sub>2</sub>, (f) 20 TPAV<sub>3</sub>/SiO<sub>2</sub> catalysts.

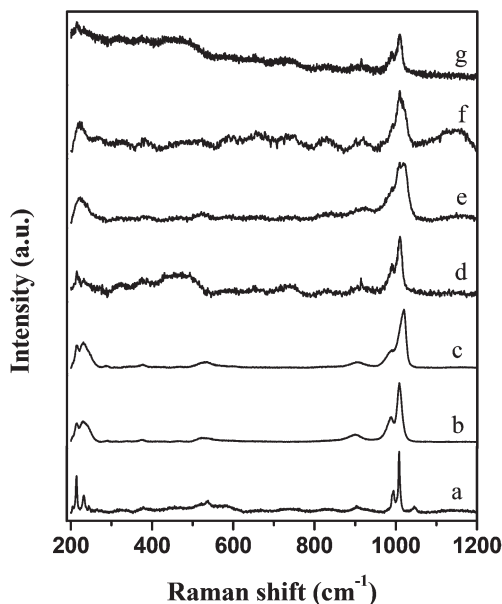


**Fig. 3** Raman spectra of (a) TPAV<sub>1</sub>, (b) TPAV<sub>2</sub>, (c) TPAV<sub>3</sub>, (d) 20 TPAV<sub>1</sub>/SiO<sub>2</sub>, (e) 20 TPAV<sub>2</sub>/SiO<sub>2</sub>, (f) 20 TPAV<sub>3</sub>/SiO<sub>2</sub> and (g) 20 TPAV<sub>1</sub>/SiO<sub>2</sub> (used) catalysts.

### 3.3. Laser Raman spectral analysis

Laser Raman spectra of catalysts are shown in Fig. 3. In the spectra of bulk TPAV<sub>x</sub> catalysts, characteristic bands related to Keggin structure were observed. The bands at 1014 and 991 cm<sup>-1</sup> can be assigned to strong W=O<sub>t</sub> symmetric and asymmetric stretching modes, respectively. The weak Raman bands at 901 and 537 cm<sup>-1</sup> can be related to asymmetric stretching vibration of bridging W-O<sub>b</sub>-W and symmetric

stretching of bridging W-O<sub>c</sub>-W. The Raman band at 242 cm<sup>-1</sup> represents the bending mode of the bridging W-O-W bonds of the intact Keggin structure. The Raman spectra of bulk TPAV<sub>x</sub> catalyst concur with those reported in the literature.<sup>27</sup> In the case of silica-supported catalysts, the Raman characteristic Keggin bands were observed showing that the Keggin structure was preserved on the support. In general, the spectra showed broad bands instead of sharp ones. The broadening denotes the presence of a strong interaction between TPAV<sub>x</sub> and the SiO<sub>2</sub> surface. The <sup>1</sup>H NMR spectra of SiO<sub>2</sub>-supported H<sub>3</sub>PW<sub>12</sub>O<sub>40</sub> (TPA) catalyst revealed that there was a strong interaction between TPA with SiO<sub>2</sub> where the protons of TPA reacted with the OH groups on silica to form -Si-OH<sub>2</sub><sup>+</sup>...H<sub>2</sub>PW<sub>12</sub>O<sub>40</sub>.<sup>45,46</sup> Similar types of interactions between TPAV<sub>x</sub> and SiO<sub>2</sub> surface might exist in the present case also. The observation of support interaction, as indicated by Raman spectroscopy, also strengthens the results obtained by XRD. Thus Raman, XRD and FT-IR results corroborate one another.

### 3.4. Temperature-programmed desorption of NH<sub>3</sub>

TPD of NH<sub>3</sub> was employed to measure the acidity of the catalysts and the patterns are shown in Fig. 4. The acidity values obtained from this study are presented in Table 1. The distribution of strong acid sites as reflected by the TPD peaks

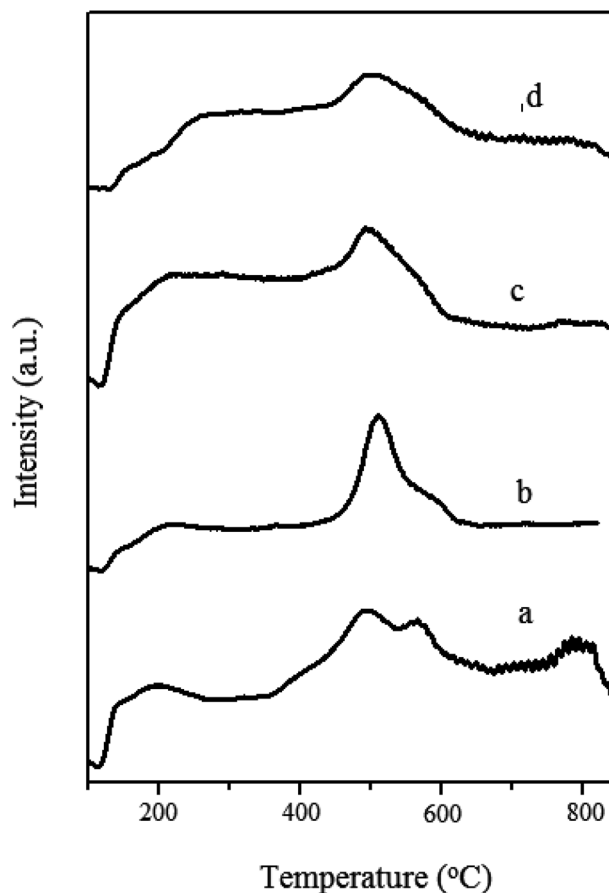


**Fig. 4** NH<sub>3</sub>-TPD pattern of (a) 20 TPA/SiO<sub>2</sub>, (b) 20 TPAV<sub>1</sub>/SiO<sub>2</sub>, (c) 20 TPAV<sub>2</sub>/SiO<sub>2</sub> and (d) 20 TPAV<sub>3</sub>/SiO<sub>2</sub> catalysts.

between 200–800 °C in the case of catalyst without vanadium indicated the strong acidity of TPA. However, substitution of vanadium for tungsten resulted in a decrease of acidic sites as well as the total acidity of the catalyst. With the substitution of more and more V ions for W there was more and more decrease in the acidity of the catalysts. From these observations one can conclude that increase in vanadium content in the primary structure of heteropoly tungstate anion decreases its acidity.

### 3.5. X-ray photoelectron spectroscopy

XPS is a versatile surface technique that can be used for chemical state analysis. Fig. 5 shows the XPS analysis of active

20 wt% TPAV<sub>1</sub>/SiO<sub>2</sub> catalyst. The binding energies of various core-electron levels (O 1s, P 2p, Si 2p, V 2p<sub>3/2</sub>, W 4f) are shown in Table 2. The Si 2p<sub>3/2</sub> peak at 104.1 eV corresponds to binding energy for SiO<sub>2</sub>.<sup>47</sup> The BE at 534 eV is assigned to oxygen of the silica support.<sup>48,49</sup> It is worth mentioning that the chemical environment of Si ions was not affected by the presence of the TPAV<sub>1</sub>. The BE of O 1s was shifted to a higher value compared to O 1s of pure TPA,<sup>50</sup> demonstrating the existence of different types of oxygen atoms in the heteropoly anion. W 4f XPS spectra displayed two peaks at 36.4 and 38.6 eV assignable to W 4f<sub>7/2</sub> and W 4f<sub>5/2</sub>, indicating the highest oxidation state of W (VI).<sup>51</sup> Generally, the W 4f

**Table 1** Acidity of TPAV<sub>x</sub>/SiO<sub>2</sub> (x = 0–3) and MPAV<sub>1</sub>/SiO<sub>2</sub> catalysts

S. no.	Catalyst	Total acidity (mmol g <sup>-1</sup> )
1	20 TPA/SiO <sub>2</sub>	0.75
2	20 TPAV <sub>1</sub> /SiO <sub>2</sub>	0.64
3	20 TPAV <sub>2</sub> /SiO <sub>2</sub>	0.46
4	20 TPAV <sub>3</sub> /SiO <sub>2</sub>	0.42
5	20 MPAV <sub>1</sub> /SiO <sub>2</sub>	0.23

**Table 2** Binding energies of core electron levels of TPAV<sub>1</sub>/SiO<sub>2</sub> catalyst

Catalyst	Binding energy (eV)				
	P 2p	O 1s	W 4f	V 2p	Si 2p
20 TPAV <sub>1</sub> /SiO <sub>2</sub> (fresh)	135.2	533.4	36.4	517.4	104.1
		534.7	38.6	519.2	
20 TPAV <sub>1</sub> /SiO <sub>2</sub> (used)	135.1	532.8	36.5	517.2	104
		534.2	38.4	518.7	

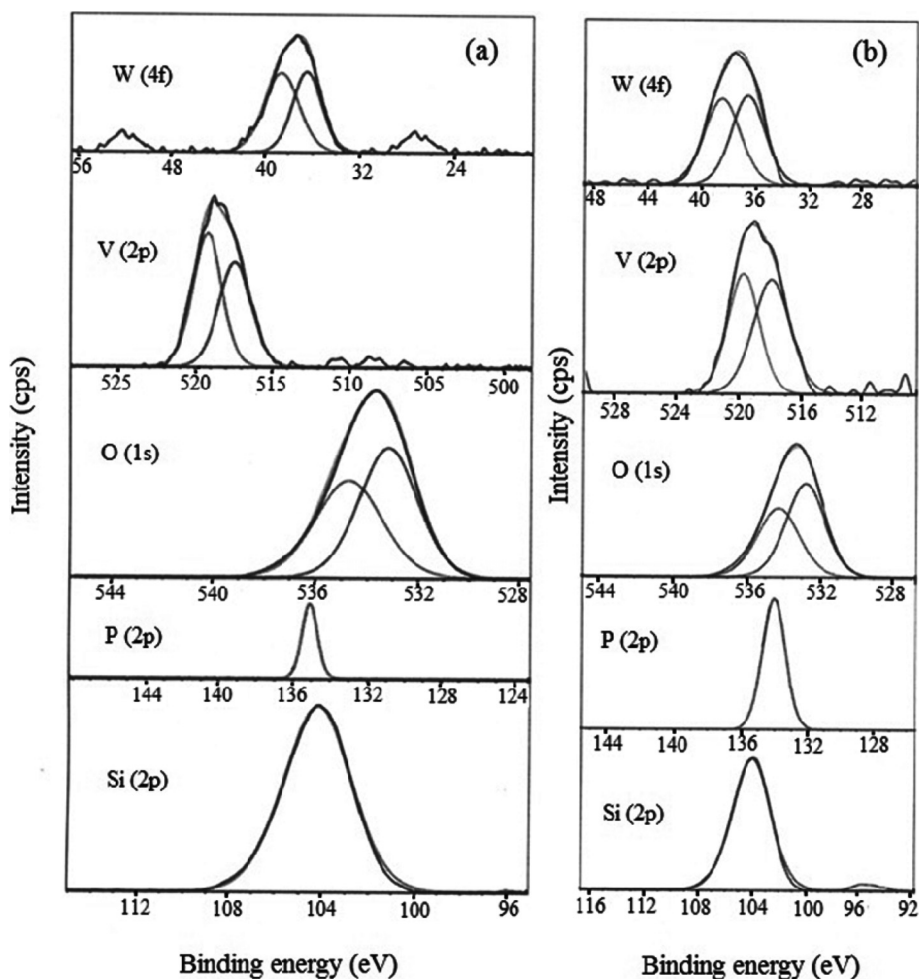


**Fig. 5** XPS spectra of (a) 20 TPAV<sub>1</sub>/SiO<sub>2</sub> (fresh) and (b) 20 TPAV<sub>1</sub>/SiO<sub>2</sub> (used) catalysts.

spectrum of TPA shows two prominent peaks at 35.8 and 37.9 eV.<sup>50</sup> Compared with bulk TPA, there was a shift of about 0.6 eV to higher BE observed for supported catalysts, indicating a change in W=O bond to W–O bond. This implies interaction of TPA with silica with the formation of W–O–Si bond. However, based on the observed Raman results, one can not rule out the possibility of interaction between W–O and Si–OH by partial proton transfer. The binding energy value of V 2p<sub>3/2</sub> core level for TPAV<sub>1</sub>/SiO<sub>2</sub> observed at 517.4 eV is a characteristic of the V<sup>5+</sup> ion.<sup>29</sup> The bulk TPAV<sub>1</sub> showed V 2p<sub>3/2</sub> binding energy at 518.1 eV (not shown). The shift of binding energy of V to a lower value in the case of TPAV<sub>1</sub>/SiO<sub>2</sub> catalyst is due to the interaction of vanadium species with support. Furthermore, P 2p exhibited a binding energy of 135 eV corresponding to the phosphorus in phosphate.<sup>52</sup> A shift in binding energy of P 2p towards a lower value by 1 eV compared to bulk TPAV<sub>1</sub> (136 eV) suggests the formation of bonding between TPAV<sub>1</sub> and the support. From the above observation, one can again conclude that the Keggin structure of TPAV<sub>1</sub> was intact and it was stabilized on SiO<sub>2</sub>.

### 3.6. Selective aerobic oxidation of benzylamine

The activity of the catalysts was evaluated for vapor-phase selective aerobic oxidation of benzylamine (BAN) at atmospheric pressure. The formation of dibenzylimine (DBI), benzonitrile (BN) and benzaldehyde (BA) was observed during the oxidation of benzylamine.

**3.6.1. Effect of vanadium content.** The TPAV<sub>x</sub>/SiO<sub>2</sub> catalysts with different V contents were studied for air oxidation of BAN and the results are shown in Fig. 6. The vanadium content in the primary structure of TPA had an influence on the oxidation of BAN. The catalyst without V (TPA/SiO<sub>2</sub>) exhibited about 50% conversion of BAN with 98% selectivity towards DBI. This result was surprising as generally very low activity in the oxidation reaction is expected due to poor oxidation ability of TPA. In addition to DBI, a trace amount of

BN was also formed. The high selectivity to DBI over TPA/SiO<sub>2</sub> might be due to the strong acidity of the catalyst. Generally, BA was also one of the oxidation products in BAN oxidation.<sup>3</sup> However, it was not detected over TPA/SiO<sub>2</sub> catalyst. Probably the BA formed during the reaction might have immediately reacted with benzylamine to form DBI.

Substitution of one V for W in the primary structure of TPA enhanced the catalytic activity. A substantial increase in conversion up to 90% was observed. The selectivity for DBI was also high. High conversion of BAN over TPAV<sub>1</sub>/SiO<sub>2</sub> catalyst is due to substitution of V for W. The change in the acid-dominated properties of TPA/SiO<sub>2</sub> catalyst towards a redox nature may be responsible for this behavior. The high redox nature of the catalyst facilitated greater conversion of BAN.

On the other hand, substitution of a higher number of vanadium atoms in heteropoly tungstate, as in the case of TPAV<sub>2</sub>/SiO<sub>2</sub> catalyst, had a different influence. The conversion of BAN decreased marginally with respect to TPAV<sub>1</sub>/SiO<sub>2</sub> catalyst. The selectivity of DBI also decreased slightly whereas selectivity of BN is increased. As more vanadium atoms were substituted in the primary structure of TPA, as in the case of TPAV<sub>3</sub>/SiO<sub>2</sub> catalyst, the conversion of BAN further decreased. At the same time, the selectivity of DBI adversely dropped and selectivity towards BN and BA was increased. It has been reported that a higher number of vanadium atoms in the primary structure leads to a decrease in acid and redox properties of the catalyst and thus reduces the activity.<sup>53</sup>

The activity profiles of TPA and TPAV<sub>x</sub> catalysts also can be explained based on the plausible mechanism shown in Scheme 1. The reaction can be assumed to proceed along the same pathway as that proposed by Neumann and Levin<sup>3</sup> for oxidative dehydrogenation of amines over vanadium-containing phosphomolybdic acid. First, BAN reacts with TPAV<sub>1</sub> to transfer two electrons and two protons to the catalyst to form its reduced state and an unstable phenylmethanimine intermediate. The reduced catalyst reacts with O<sub>2</sub> in air to reoxidize into the original state with the release of a water molecule as a byproduct. There are two possible pathways for the formation of DBI. In one path (route 1), the unstable intermediate phenylmethanimine reacts with another molecule of BAN to form aminal and thereby releases an NH<sub>3</sub> molecule to form the coupled product. A similar observation was also made by Wang and co-workers<sup>16</sup> over photo-catalytically active mesoporous graphite carbon nitride (mpg-C<sub>3</sub>N<sub>4</sub>)-catalyzed oxidative coupling of amines. On the other hand, it can also be formed by the hydrolysis of phenylmethanimine to BA, which subsequently reacts with available BAN (route 2). The formation of BN is a result of further oxidation of phenylmethanimine intermediate and reduction of the catalyst.

In order to support the proposed mechanism on TPAV<sub>1</sub>/SiO<sub>2</sub>, the activity of this catalyst was compared with that of vanadium-substituted molybdophosphoric acid supported on silica (MPAV<sub>1</sub>/SiO<sub>2</sub>). The MPAV<sub>1</sub>/SiO<sub>2</sub> catalyst was studied for this reaction by anticipating a high oxidation ability of MPAV<sub>1</sub> compared to TPAV<sub>1</sub>. The comparative activity results are shown in Fig. 7. As expected, MPAV<sub>1</sub>/SiO<sub>2</sub> catalyst exhibited almost

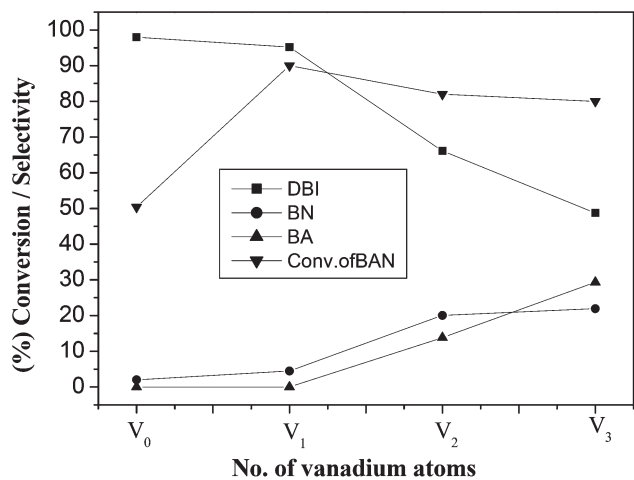
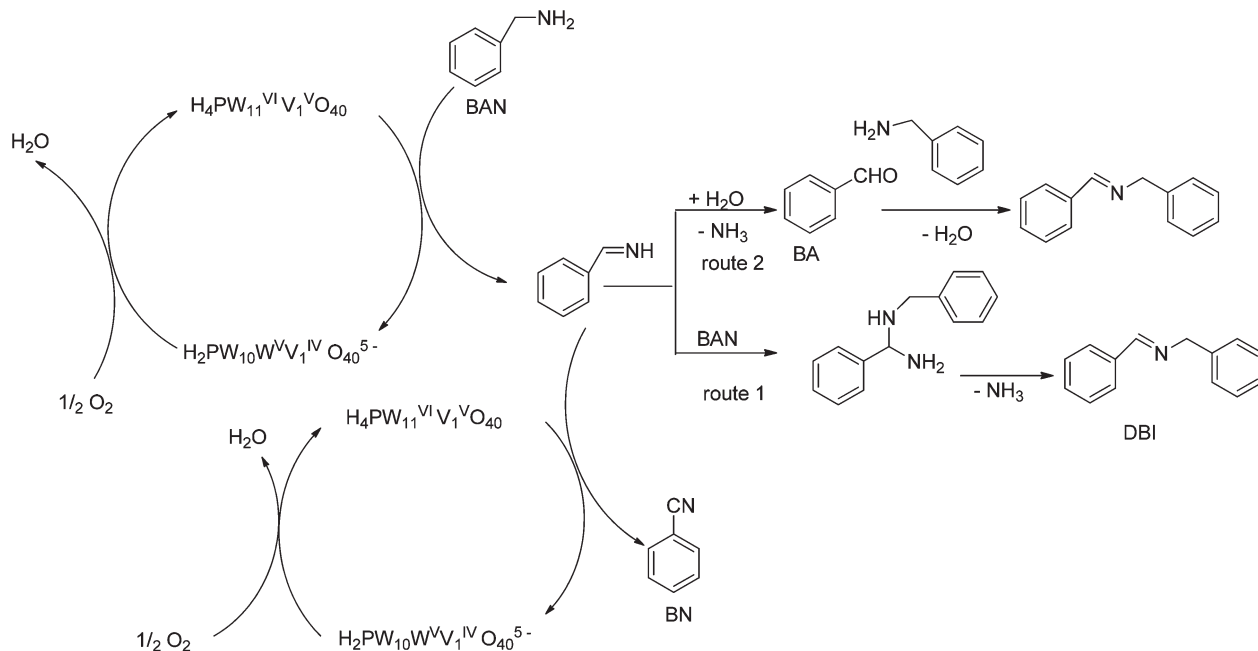


**Fig. 6** Effect of vanadium content in TPAV<sub>x</sub>/SiO<sub>2</sub> catalyst on the catalytic oxidation of benzylamine (reaction conditions: catalyst mass = 0.5 g, reactant mole ratio = 1 : 7.9 (BAN/air), GHSV = 2688 h<sup>-1</sup>).



Scheme 1 Plausible reaction mechanism.

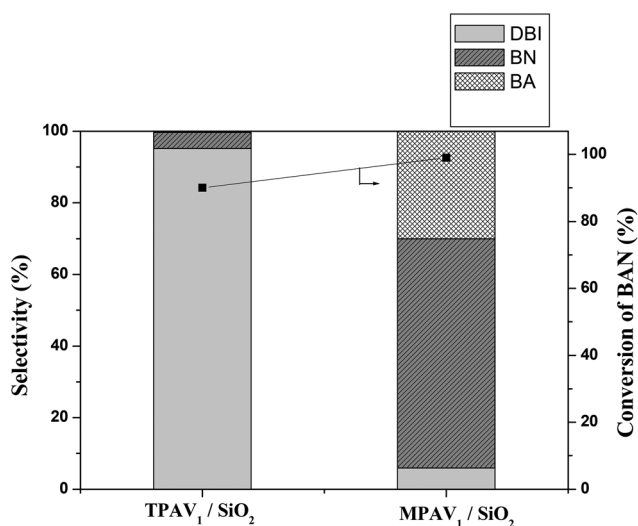


Fig. 7 Comparison of TPAV<sub>1</sub>/SiO<sub>2</sub> and MPAV<sub>1</sub>/SiO<sub>2</sub> catalysts for the oxidation of benzylamine (reaction conditions: catalyst mass = 0.5 g, reactant mole ratio = 1 : 7.9 (BAN/air), GHSV = 2688 h<sup>-1</sup>).

complete conversion of BAN and with varied selectivity. The formation of DBI was less whereas the selectivity towards BN and BA was high. Among the Keggin type of heteropoly acids molybdophosphoric acid (MPA) is quite often used as an oxidation catalyst due to high oxidation ability of Mo. Substitution of a more redox active element like V for Mo in the Keggin framework of MPA enhances the redox nature of the catalyst further.<sup>19</sup>

It is anticipated that the formation of a higher amount of DBI over TPAV<sub>1</sub>/SiO<sub>2</sub> catalyst was influenced by the acidity of

the catalyst. There are two possible competitive reactions that can take place over these catalysts after the initial oxidative dehydrogenation of BAN, *i.e.* hydrolysis of phenylmethanimine and attack of imine by BAN (Scheme 1). Since no formation of BA was observed over silica-supported TPA and TPAV<sub>1</sub> catalysts, it indicates that the reaction can be assumed to proceed through route 1. NH<sub>3</sub>-TPD measurements (Table 1) reveal that TPA and TPAV<sub>1</sub> catalysts exhibit strong acidity that could assist the nucleophilic attack of amine at the C=N bond of imine to form aminal, which loses ammonia to form DBI. On the other hand, the reaction is also implied to proceed through route 2, however control experiments under the same reaction conditions by feeding BA and BAN over these oxidation catalysts in the absence of air resulted in no significant quantity of BA and BAN and exclusive formation of DBI was observed. It is demonstrated that acidity of the catalyst did not influence the formation of DBI from BA and BAN. Thus, high selectivity of DBI for 20 TPAV<sub>1</sub>/SiO<sub>2</sub> catalyst is significantly controlled by the rate of the two successive oxidative dehydrogenation steps leading to BN formation (Scheme 1) which are mainly dependent on the rate of desorption. The quicker they are, the lower is the selectivity to the competitive reaction of DBI formation over these catalysts.

**3.6.2. Effect of reaction temperature.** The influence of reaction temperature on the conversion and selectivity for BAN oxidation was studied over the most active TPAV<sub>1</sub>/SiO<sub>2</sub> catalyst. The activity results are shown in Fig. 8. The initial temperature of the reaction was higher than the boiling point of the substrate. The conversion of BAN increased with increase in reaction temperature. However, the selectivity to DBI was consistent up to 220 °C and decreased thereafter. The decrease in selectivity for DBI at high reaction temperature appeared to be

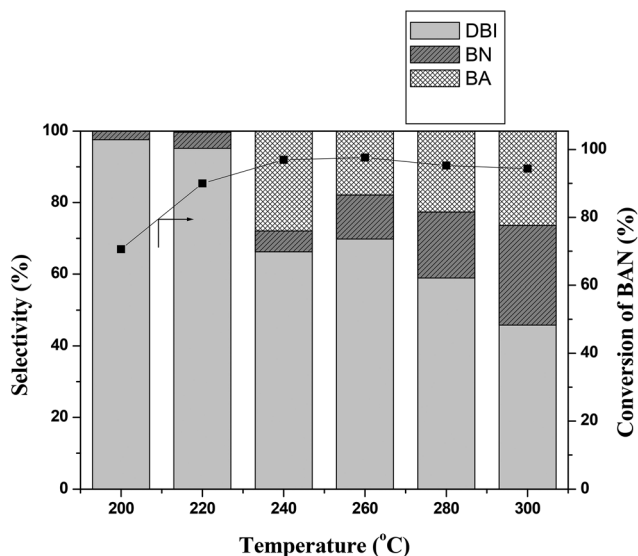


**Fig. 8** Effect of reaction temperature on oxidation of benzylamine over 20 TPAV<sub>1</sub>/SiO<sub>2</sub> (reaction conditions: catalyst mass = 0.5 g, reactant mole ratio = 1 : 7.9 (BAN/air), GHSV = 2688 h<sup>-1</sup>).

compensated by the increase in formation of BN and BA. Though the optimum temperature for this reaction was 220 °C, the results suggest that it is possible to achieve a better activity profile even at low reaction temperature under vapor-phase conditions.

**3.6.3. Thermal stability of TPAV<sub>1</sub>/SiO<sub>2</sub> catalyst.** In order to understand the thermal stability of 20 wt% TPAV<sub>1</sub>/SiO<sub>2</sub> catalyst, *in situ* Raman studies were carried over the freshly prepared catalysts (uncalcined) and the results are presented in Fig. 9. At room temperature, the strong Raman band observed at 1008 cm<sup>-1</sup> can be attributed to symmetric stretching of the tungsten-terminal oxygen (W=O<sub>t</sub>) within WO<sub>6</sub> octahedra of TPAV<sub>1</sub>/SiO<sub>2</sub> catalyst. Since the vibrations of the W=O<sub>t</sub> strongly depend on water molecules coordinated to heteropoly anion, a shift in the peak position from 1008 cm<sup>-1</sup> towards 1027 cm<sup>-1</sup> was observed when the sample was exposed to 200 °C due to loss of crystal water.<sup>54</sup> Such a vibrational shift of W=O<sub>t</sub> is reported in the literature upon dehydration of bulk TPAV<sub>1</sub>.<sup>27</sup> The water molecules were removed upon calcination at 300 °C leaving dehydrated proton H<sup>+</sup> species and keeping the primary structure of TPAV<sub>1</sub> intact. Thereafter, no significant shift in peak positions upon further calcination up to 400 °C was observed. This indicates that the Keggin structure of TPAV<sub>1</sub> remained stable on SiO<sub>2</sub>. Decomposition of TPAV<sub>1</sub> was observed at 500 °C, as indicated by a decrease in the intensity of the main peak at 1027 cm<sup>-1</sup>. On further increase in temperature up to 600 °C, two new broad bands appeared around 799 cm<sup>-1</sup>. These bands became sharper with increasing temperature leading to formation of crystalline WO<sub>3</sub> species.<sup>55</sup> However, when bulk TPAV<sub>1</sub> was calcined above 300 °C, segregation of vanadium from the primary structure of TPA was noticed (data not shown).<sup>27</sup> On the other hand, the supported catalyst was stable up to 400 °C. Therefore, *in situ* Raman studies explain the thermal stability of TPAV<sub>1</sub>/SiO<sub>2</sub> catalyst and

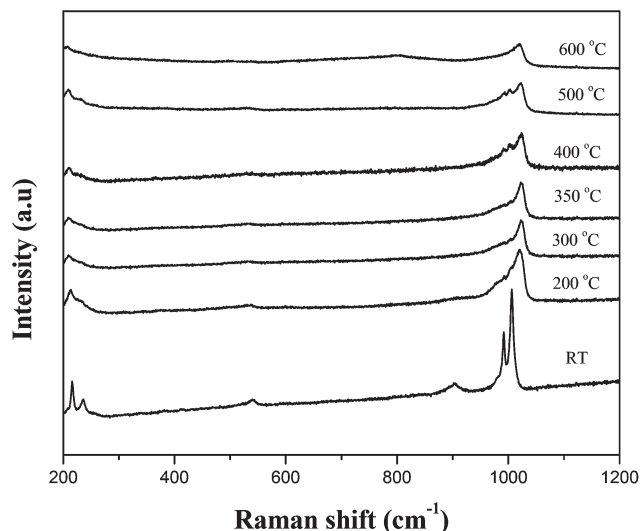


**Fig. 9** *In situ* Raman spectra of 20 TPAV<sub>1</sub>/SiO<sub>2</sub> catalyst as a function of treatment temperature.

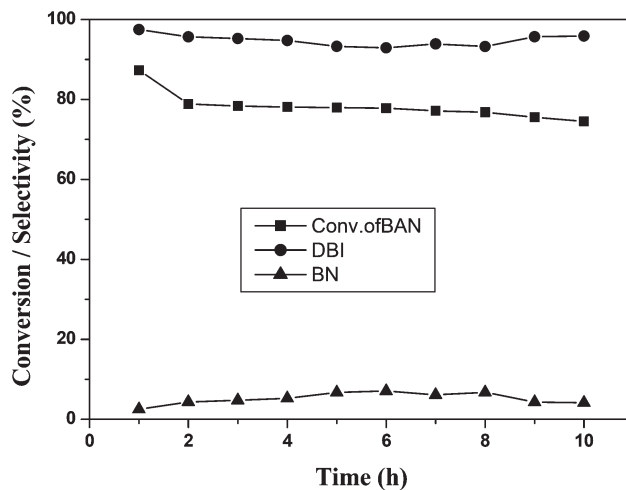


**Fig. 10** Time-on-stream analysis over 20 TPAV<sub>1</sub>/SiO<sub>2</sub> catalyst at a reaction temperature of 220 °C (reaction conditions: catalyst mass = 0.5 g, reactant mole ratio = 1 : 7.9 (BAN/air), GHSV = 2688 h<sup>-1</sup>).

also infer that the Keggin structure of TPAV<sub>1</sub> is thermally stable under the present reaction conditions.

**3.6.4. Time-on-stream analysis.** The time-on-stream analysis was performed over 20 TPAV<sub>1</sub>/SiO<sub>2</sub> catalyst at a fixed reaction temperature (220 °C) to know the stability of the catalyst. The resultant profile is shown in Fig. 10. In the first one hour, the activity of the catalyst was very high and decreased slightly during the second hour. Thereafter, consistent activity was observed for a period of 8 h. However, the selectivity of DBI was not disturbed during the entire course of the reaction. The consistent catalytic activity of TPAV<sub>1</sub> can be due to the intact Keggin structure on SiO<sub>2</sub>. *In situ* Raman analysis reveals that the catalyst was thermally stable up to 400 °C. After the reaction, the spent catalyst was characterized by XRD, FT-IR,

Raman and XPS analysis. The spectral pattern of used catalyst was compared to that of the virgin catalyst. The spectra of spent catalyst did not differ from that of fresh catalyst. These results also divulge that the Keggin structure of TPAV<sub>1</sub> remains unaltered after the reaction.

## 4. Conclusions

A highly efficient and selective catalyst for vapor-phase aerobic oxidation of benzylamine to dibenzylimine was demonstrated. FT-IR, Raman and XPS results suggested the incorporation of vanadium into the primary structure of heteropoly tungstate. There was a strong interaction of TPAV<sub>1</sub> with the surface of silica. The presence of vanadium in the primary structure of heteropoly tungstate enhances the catalytic activity and selectivity due to controllable acidity and the redox nature of the catalyst. The catalyst is highly active for the oxidation of primary amine (benzylamine). *In situ* Raman and time-on-stream studies reveal that the catalyst is stable and exhibits consistent activity.

## Acknowledgements

The authors KTVR and BHB thank the Council of Scientific and Industrial Research (CSIR), New Delhi, for the award of senior and junior research fellowships, respectively.

## References

- J. Gawronski, N. Wascinska and J. Gajewy, *Chem. Rev.*, 2008, **108**, 5227.
- K. C. Nicolaou, C. J. N. Mathison and T. Montagnon, *J. Am. Chem. Soc.*, 2004, **126**, 5192.
- R. Neumann and M. Levin, *J. Org. Chem.*, 1991, **56**, 5707.
- B. Zhu and R. J. Angelici, *Chem. Commun.*, 2007, 2157.
- B. Zhu, M. Lazar, B. G. Trewyn and R. J. Angelici, *J. Catal.*, 2008, **260**, 1.
- L. Aschwanden, B. Panella, P. Rossbach, B. Keller and A. Baiker, *ChemCatChem*, 2009, **1**, 111.
- A. Grirrane, A. Corma and H. Garcia, *J. Catal.*, 2009, **264**, 138.
- M.-H. So, Y. Liu, C.-M. Ho and C.-M. Che, *Chem.-Asian J.*, 2009, **4**, 1551.
- A. Prades, E. Peris and M. Albrecht, *Organometallics*, 2011, **30**, 1162.
- G. Chu and C. Li, *Org. Biomol. Chem.*, 2010, **8**, 4716.
- S. Kodama, J. Yoshida, A. Nomoto, Y. Ueta, S. Yano, M. Ueshima and A. Ogawa, *Tetrahedron Lett.*, 2010, **51**, 2450.
- R. D. Patil and S. Adimurthy, *Adv. Synth. Catal.*, 2011, **353**, 1695.
- J.-R. Wang, Y. Fu, B.-B. Zhang, X. Cui, L. Liu and Q.-X. Guo, *Tetrahedron Lett.*, 2006, **47**, 8293.
- X. Lang, H. Ji, C. Chen, W. Ma and J. Zhao, *Angew. Chem., Int. Ed.*, 2011, **50**, 3934.
- S. Furukawa, Y. Ohno, T. Shishido, K. Teramura and T. Tanaka, *ACS Catal.*, 2011, **1**, 1150.
- F. Su, S. C. Mathew, L. Mohlmann, M. Antonietti, X. Wang and S. Blechert, *Angew. Chem., Int. Ed.*, 2011, **50**, 657.
- A. Dhakshinamoorthy, M. Alvaro and H. Garcia, *ChemCatChem*, 2010, **2**, 1438.
- W. F. Hoelderich and F. Kollmer, *Pure Appl. Chem.*, 2000, **72**, 1273.
- I. V. Kozhevnikov, *Chem. Rev.*, 1998, **98**, 171.
- N. Mizuno and M. Misono, *Chem. Rev.*, 1998, **98**, 199.
- A. Brückner, G. Scholz, D. Heidemann, M. Schneider, D. Herein, U. Bentrup and M. Kant, *J. Catal.*, 2007, **245**, 369.
- N. Lingaiah, K. Mohan Reddy, P. Nagaraju, P. S. Sai Prasad and I. E. Wachs, *J. Phys. Chem. C*, 2008, **112**, 8294.
- M. Kanno, T. Yasukawa, W. Ninomiya, K. Ooyachi and Y. Kamiya, *J. Catal.*, 2010, **273**, 1.
- T. Ressler, U. Dorn, A. Walter, S. Schwarz and A. H. P. Hahn, *J. Catal.*, 2010, **275**, 1.
- S. Benadji, P. Eloy, A. Leonard, B. L. Su, K. Bachari, C. Rabia and E. M. Gaigneaux, *Microporous Mesoporous Mater.*, 2010, **130**, 103.
- K. T. Venkateswara Rao, P. S. N. Rao, P. Nagaraju, P. S. Sai Prasad and N. Lingaiah, *J. Mol. Catal. A: Chem.*, 2009, **303**, 84.
- N. Lingaiah, J. E. Molinari and I. E. Wachs, *J. Am. Chem. Soc.*, 2009, **131**, 15544.
- D. Ryul Park, S. H. Song, U. G. Hong, J. G. Seo, J. C. Jung and I. K. Song, *Catal. Lett.*, 2009, **132**, 363.
- K. Yonehara, K. Kamata, K. Yamaguchi and N. Mizuno, *Chem. Commun.*, 2011, **47**, 1692.
- A. S. H. Kumar, K. T. Venkateswara Rao, K. Upendar, Ch. Sailu, N. Lingaiah and P. S. Sai Prasad, *Catal. Commun.*, 2012, **18**, 37.
- K. T. Venkateswara Rao, P. S. Sai Prasad and N. Lingaiah, *Green Chem.*, 2012, **14**, 1507.
- K. T. Venkateswara Rao, B. Haribabu, P. S. Sai Prasad and N. Lingaiah, *ChemCatChem*, 2012, **4**, 1173.
- Ch. R. Kumar, K. Jagadeeswaraiyah, P. S. Sai Prasad and N. Lingaiah, *ChemCatChem*, 2012, **4**, 1360.
- N. Lingaiah, N. Seshu Babu, K. Mohan Reddy, P. S. Sai Prasad and I. Suryanarayana, *Chem. Commun.*, 2007, 278.
- P. Nagaraju, N. Pasha, P. S. Sai Prasad and N. Lingaiah, *Green Chem.*, 2007, **9**, 1126.
- P. S. N. Rao, K. T. Venkateswara Rao, P. S. Sai Prasad and N. Lingaiah, *Catal. Commun.*, 2010, **11**, 547.
- G. A. Tsigdinos and C. J. Hallada, *Inorg. Chem.*, 1968, **7**, 437.
- Y. Zhang, Z. Du and E. Min, *Catal. Today*, 2004, **93–95**, 327.
- S. Shinach, M. Matsushita, K. Yamaguchi and N. Mizuno, *J. Catal.*, 2005, **233**, 81.
- C. Rocchiccioli-Deltcheff and M. Fournier, *J. Chem. Soc., Faraday Trans.*, 1991, **87**, 3913.

- 41 D. Casarini, G. Centi, P. Jiru, V. Lena and Z. Tvaruzkova, *J. Catal.*, 1993, **143**, 325.
- 42 K. N. Rao, R. Gopinath, M. S. Kumar, I. Suryanarayana and P. S. S. Prasad, *Chem. Commun.*, 2001, 2088.
- 43 Ch. Ramesh Kumar, K. T. Venkateswara Rao, P. S. Sai Prasad and N. Lingaiah, *J. Mol. Catal. A: Chem.*, 2011, **337**, 17.
- 44 G. D. Yadav and G. George, *Catal. Today*, 2009, **141**, 130.
- 45 N. Legagneux, J.-M. Basset, A. Thomas, F. Lefebvre, A. Goguet, J. Sa and C. Hardacre, *Dalton Trans.*, 2009, 2235.
- 46 A. D. Newman, D. R. Brown, P. Siril, A. F. Lee and K. Wilson, *Phys. Chem. Chem. Phys.*, 2006, **8**, 2893.
- 47 V. L. Parola, G. Deganello, C. R. Tewell and A. M. Venezia, *Appl. Catal., A*, 2002, **235**, 171.
- 48 S. Benadji, P. Eloy, A. Leonard, B.-L. Su, C. Rabia and E. M. Gaigneaux, *Microporous Mesoporous Mater.*, 2012, **154**, 153.
- 49 R. S. Araujo, D. C. S. Azevedo, E. Rodriguez-Castellon, A. Jimenez-Lopez and C. L. Cavalcante Jr., *J. Mol. Catal. A: Chem.*, 2008, **281**, 154.
- 50 P. A. Jalil, M. Faiz, N. Tabet, N. M. Hamdan and Z. Hussain, *J. Catal.*, 2003, **217**, 292.
- 51 I. V. Kozhevnikov, S. Holmes and M. R. H. Siddiqui, *Appl. Catal., A*, 2001, **214**, 47.
- 52 A. Predoeva, S. Damyanova, E. M. Gaigneaux and L. Petrov, *Appl. Catal., A*, 2007, **319**, 14.
- 53 G. Mestl, T. Ilkenhans, D. Spielbauer, M. Dieterle, O. Timpe, J. Kröhnert, F. Jentoft, H. Knözinger and R. Schlögl, *Appl. Catal., A*, 2001, **210**, 13.
- 54 G. M. Brown, M. R. Noe-Spirlet, W. R. Busing and H. A. Levy, *Acta Crystallogr., Sect. B: Struct. Crystallogr. Cryst. Chem.*, 1977, **33**, 1038.
- 55 M. Scheithauer, R. K. Grasselli and H. Knozinger, *Langmuir*, 1998, **14**, 3019.